Photophysics and Photochemistry of Horseradish Peroxidase A2 upon Ultraviolet Illumination

Maria Teresa Neves-Petersen,* Søren Klitgaard,* Ana Sofia Leitão Carvalho,† Steffen B. Petersen,* Maria Raquel Aires de Barros,‡ and Eduardo Pinho e Melo‡§

*Department of Physics and Nanotechnology, NanoBiotechnology Section, UltrafastBioSpectroscopy Group, Aalborg University, Aalborg, Denmark; †Institute of Molecular Pathology and Immunology of the University of Porto, 4200 Porto, Portugal; ‡Biological Engineering Research Group, Instituto Superior Técnico, 1049-001 Lisbon, Portugal; and §Center of Structural and Molecular Biomedicine, Universidade do Algarve, Campus de Gambelas, 8005-139 Faro, Portugal

ABSTRACT Detailed analysis of the effects of ultraviolet (UV) and blue light illumination of horseradish peroxidase A2, a heme-containing enzyme that reduces H_2O_2 to oxidize organic and inorganic compounds, is presented. The effects of increasing illumination time on the protein's enzymatic activity, Reinheitzahl value, fluorescence emission, fluorescence lifetime distribution, fluorescence mean lifetime, and heme absorption are reported. UV illumination leads to an exponential decay of the enzyme activity followed by changes in heme group absorption. Longer UV illumination time leads to lower T_m values as well as helical content loss. Prolonged UV illumination and heme irradiation at 403 nm has a pronounced effect on the fluorescence quantum yield correlated with changes in the prosthetic group pocket, leading to a pronounced decrease in the heme's Soret absorbance band. Analysis of the picosecond-resolved fluorescence emission of horseradish peroxidase A2 with streak camera shows that UV illumination induces an exponential change in the preexponential factors distribution associated to the protein's fluorescence lifetimes, leading to an exponential increase of the mean fluorescence lifetime. Illumination of aromatic residues and of the heme group leads to changes indicative of heme leaving the molecule and/or that photoinduced chemical changes occur in the heme moiety. Our studies bring new insight into light-induced reactions in proteins. We show how streak camera technology can be of outstanding value to follow such ultrafast processes and how streak camera data can be correlated with protein structural changes.

INTRODUCTION

Peroxidases are heme-containing enzymes that reduce H_2O_2 to oxidize a wide variety of organic and inorganic compounds. The heme prosthetic group, appointed ''ferriprotoporphyrin IX'', allows electron transfer between reductant and oxidant substrates (1). During catalysis in plant peroxidases a porphyrin cation π radical is formed (2), and in yeast cytochrome *c* peroxidase a tryptophan radical plays the equivalent role (3,4). In both cases in the first reaction step the iron ion becomes hexacoordinated to an oxygen atom (Fe^{IV}=O). In classical plant peroxidases tryptophan is uniquely represented and is highly conserved, located in a surface loop connecting two helices. The indole ring is directed toward the core of the protein lying above the plane defined by the heme group at an average distance of 16–18 Å (5–8) (Fig. 1 *A*). Trp fluorescence in classical plant peroxidases is highly quenched in the native state due to energy transfer from the excited state of tryptophan to the heme group (5,9,10). Quantum yields are 100 orders of magnitude lower than that of tryptophan free in solution. Ferriprotoporphyrin also displays a visible absorption spectrum.

The most important UV light absorbers in proteins are the aromatic residues, Trp, Tyr, and Phe along with cystine and His (11). It is known that tryptophan and tyrosine radicals can be induced by ultraviolet (UV) illumination (12–14). Heme groups are also excellent UV absorbers. UV illumination might in some cases induce enzyme inactivation (15–18). The mechanisms of inactivation are believed to be due to ionization of aromatic residues associated with an electron transfer mechanism and radical formation together with disruption of disulphide bridges (19–23). Earlier studies confirm that the major reaction after UV excitation of enzymes is photoionization (24). The excited tryptophan after photoionization gives $TrpH^+$, and electron is ejected from the molecule. In heme proteins, the $TrpH^+$ might reduce the ferrous heme (25). Porphyrins are a major source of free radicals and singlet oxygen and can induce photobleaching in fluorescent molecules (26). Several studies are reported on photoinactivation of catalase, a tetrameric heme-containing enzyme. Catalase degrades H_2O_2 to oxygen and water and represents an important part of the antioxidative system in cells. Blue light (380–500 nm) illumination of sunflower catalase causes partial heme destruction, and oxidation of histidine, present in the catalytic center of catalase, perhaps is an early event in photoinactivation (27). UV irradiation (365 nm) of bovine liver catalase leads to the formation of catalytically inactive compounds III (oxyferrous catalase) and II (catalase FeIV) (28). UV C irradiation of flavocytochrome b_2, which houses a heme prosthetic group, results in enzyme inactivation, where Trp and Tyr residues as well as the heme group are modified (25). Oxygen presence offers protection of tryptophan against UV-induced damage due to quenching (11), whereas the heme group can act as a photosensitizer thus generating harmful singlet oxygen (29).

Submitted August 21, 2006, and accepted for publication November 27, 2006.

Address reprint requests to Maria Teresa Neves-Petersen, E-mail: tnp@nanobio.aau.dk.

0006-3495/07/03/2016/12 $2.00

doi: 10.1529/biophysj.106.095455

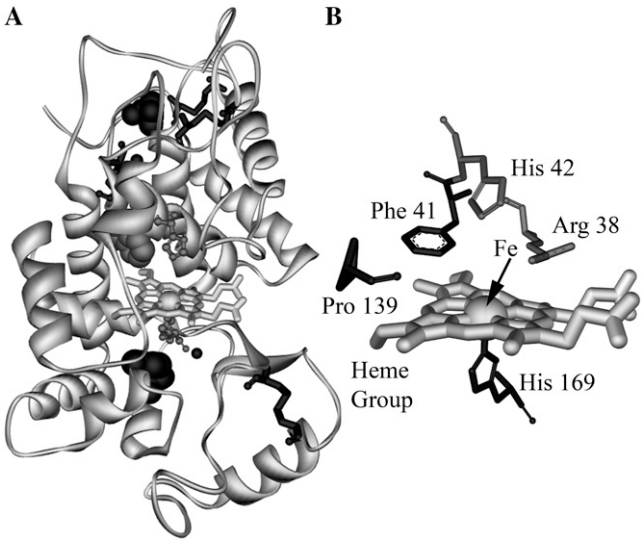

FIGURE 1 (*A*) Three-dimensional representation of the x-ray crystal structure of *A. thaliana* peroxidase A2 orthologous for HRPA2 showing 95% homology (Brookhaven accession code 1PA2). The heme group (*central white stick* representation) is located between the distal and proximal domains, which each contain one calcium atom (shown as *small black spheres*). The heme iron (*white*, Corey-Pauling-Koltun, CPK, representation) in the heme group is complexed to a His residue (*gray ball* and *stick* representation). Two more histidines are located in the distal domain. Three cystines (*black sticks* representation) are located in the distal domain along with one Tyr residue (*black* CPK representation). The tryptophan residue (*gray* CPK representation) is located close to the heme group with its indole ring. The proximal domain contains the fourth cystine and a Tyr residue near the calcium ion. (*B*) Schematic representation of the heme cavity in Arabidopsis ATP A2, showing relative disposition of His-42 and Arg-38 residues near the distal side of the heme (59).

This work presents a detailed spectroscopic analysis of UV-induced changes in secondary structure, enzymatic activity, fluorescence emission, fluorescence lifetime distribution, fluorescence mean lifetime, and heme absorption of horseradish peroxidase A2 (HRPA2). The catalytic activity, conformational changes at the secondary structure level, protein fluorescence, and heme absorption were monitored after Trp 296-nm UV illumination. A streak camera study on the effects of UV illumination time on the distribution of the two shortest fluorescence lifetimes of the single endogenous aromatic residue Trp in HRPA2, at pH 4, is presented. We also highlight the outstanding value of streak camera technology in following ultrafast processes and show how streak camera data can be correlated with protein structural changes. Also, we hereby present the effects of continuous illumination of the heme group at 403 nm on Trp fluorescence emission and on heme absorption bands.

MATERIALS AND METHODS

Chemicals and sample preparation

Horseradish peroxidase was obtained from Biozyme Laboratories (Blaenavon, UK) (labeled HRP-5) as lyophilized salt-free powder and used without further purification. HRP-5 corresponds to HRPA2 according to the nomenclature of Shannon et al. (30) and data reported by Hiner et al. (31). The degree of purity was checked by sodium dodecylsulfate-polyacrylamide gel electrophoresis, and a single band was observed when stained with Coomassie. HRPA2 concentrations were determined considering the molar extinction coefficient $\varepsilon_{403\text{nm}} = 100\ \text{mM}^{-1}\text{cm}^{-1}$ (32). Protein solutions used for spectroscopic studies were dissolved in buffer made with Milli-Q water. All salts were of analytical grade. Acetate buffer was used for pH 4. Buffer concentration was always 25 mM.

Extinction coefficient as a function of wavelength of HRPA2 and hematin

The absorbance from 250 nm to 700 nm of a horseradish peroxidase solution prepared as mentioned above was measured on a Thermo Electron (Waltham, MA) UV1 spectrophotometer and compared with a study performed by Du et al. (33) on the absorption of hematin in acetic acid.

Tryptophan irradiation-steady-state fluorescence

The enzyme solution (3 mL of a 5 μM protein solution) was continuously irradiated for different time periods at 296 nm using a 75 W Xenon arc lamp from an RTC 2000 PTI (Photon Technology International, Birmingham, NJ) spectrometer provided with a monochromator. Excitation and emission slit widths were set to 6 nm. Tryptophan fluorescence was monitored at 350 nm (excitation spectra) and excited at 296 nm (emission spectra). Temperature in the cell, a quartz cuvette (1-cm path length) was controlled using a Peltier element. The sample was continuously stirred at 650 rpm to maintain the homogeneity of the solution, and the temperature was kept constant at 20°C. Line voltage was controlled and maintained at 4 V, thus avoiding fluctuations deriving from the power coming from the electrical outlet.

The fluorescence emission curve as a function of illumination time (displayed in Fig. 3 *A*) was fitted to a biexponential function like the one described by Eq. 1,

$$IF(t) = C_1 + C_2\exp(-k_i t) + C_3\exp(-k_d t), \qquad (1)$$

where $IF(t)$ is the intensity of the fluorescence measured at time, t; k_i and k_d are the rate constants for the increase and decrease of the fluorescence intensity, respectively; and C_i ($i = 1$, 2, or 3) are constants.

Activity measurements, steady-state fluorescence spectra, far-UV circular dichroism (CD) spectra, and denaturation curves after ellipticity at 223 nm were determined for samples irradiated for different time periods. Control samples, without irradiation, underwent the same treatment as the exposed ones.

Activity measurements

HRPA2 activity was measured at room temperature using 50 mM guaiacol in 25 mM acetate buffer (pH 4) and 4.4 mM H_2O_2. The reaction was followed for 1 min by reading the increase in absorbance at 470 nm. The extinction coefficient of the oxidation product, $\varepsilon_{470\text{nm}} = 26.6\ \text{mM}^{-1}\text{cm}^{-1}$, was used to calculate initial velocities.

Far-UV CD measurements

CD measurements were carried out using a Jasco (Tokyo, Japan) spectropolarimeter, model J-715. The ellipticity values were obtained in mdegrees directly from the instrument and converted to the mean residue ellipticity Θ_{MRW} as previously stated (8). The far-UV CD spectra were measured using a rectangular quartz cell of 1-mm path length. Each spectrum was an average of six scans between 300 and 200 nm. The resultant ellipticities of the HRPA2 solutions were calculated by subtracting the ellipticity of the buffer

solution. The wavelength of 223 nm was used to monitor thermal denaturation in the far-UV CD range. Temperature scans were carried out in the temperature range 293–358 K using a Peltier element (irradiated samples) or a thermostated cuvette by means of a circulating water bath, and a temperature probe was immersed in the protein (dark control samples). The experimental parameters were as follows: 1-nm bandwidth, 0.2-K step resolution, 2-s response time, and scanning rates 1.5 (irradiated samples) and 2.6 K min^{-1} (control).

HRPA2 heme irradiation studies

Irradiation and steady-state fluorescence

A total of 3 mL of a 4 μM protein solution was continuously irradiated for 30 h at 403 nm using a 75-W Xenon arc lamp from a RTC 2000 PTI (Photon Technology International) spectrometer provided with a monochromator (slits width 6 nm). Temperature in the cell, a quartz cuvette (1-cm path length) was controlled using a Peltier element and was kept constant at 298 K. The sample was continuously stirred at 650 rpm to maintain the homogeneity of the solution. Line voltage was controlled and maintained at 4 V, thus avoiding fluctuations deriving from the power coming from the electrical outlet. Before 403 nm irradiation and at specified times during the irradiation, tryptophan fluorescence emission intensity at 350 nm upon 296-nm excitation was acquired.

Irradiation and absorption measurements

In another experiment, absorption by the protein solution was monitored before and after irradiation with 403-nm light for 26 h. The sample was irradiated using the same conditions as above. Measurements were performed on a Thermo Electron UV1 spectrophotometer.

Time-resolved lifetime measurements—a streak camera study

Time-resolved measurements were carried out upon exciting the samples with ultrashort UV laser pulses at 280 nm and 290 nm (for selective excitation of Trp residue). The 280-nm excitation light was generated by sending the output from a Spectra Physics (Mountain View, CA) Tsunami laser (<100-fs pulse duration, 12-nm fullwidth at half-maximum, 80-MHz repetition rate, $\lambda = 840$ nm, Tsunami 3960, Spectra Physics pumped by a high power (5 W at 532 nm) Millennia V solid state laser, Spectra Physics) through a pulse picker, which decreased the pulse repetition rate to 8 MHz. The fundamental pulse (840 nm) was mixed with its second harmonic (420 nm) in a frequency doubler/tripler unit (GWU-Lasertechnik, Erfstadt, Germany) to generate pulses at 280 nm. The power at 280 nm was 0.290 mW. The 290-nm excitation light was generated by tuning the Spectra Physics Tsunami laser to 870 nm. After the pulse picker, the fundamental pulse (870 nm) was mixed with its second harmonic (435 nm) in a frequency doubler/tripler unit (GWU-Lasertechnik) to generate pulses at 290 nm. The power at 290 nm was 0.216 mW. The sample was placed in a 1400-μL quartz cuvette and excited along the 1-cm light path. The cuvette was placed in front of the input slit (100 μm) of a spectrograph (Oriel, Darmsdadt, Germany, MS257, with a grating blazed at 400 nm with 600 lines/mm), after which it was focused into the slit of the input optics (100-μm slit) of the streak camera (Optronis, Kehl, Germany).

The sample was continuously irradiated with the 280-nm and 290-nm excitation light. Sample concentration was 49 μM. The different illumination times were 0, 34, 52, 67, 84, 106, 122, 137, and 152 min for the 280-nm series and from 0 to 170 min every 10 min for the 290-nm series. Fluorescence emission was followed in a time window of ~1.65 ns after excitation. The fluorescence lifetimes of horseradish peroxidase (HRP) were assumed to remain the same independent of illumination time, whereas the preexponential factors were assumed to change, thus enabling a global analysis approach (see note below regarding global analyses). The governing equations for the time-resolved intensity decay data were assumed to be a sum of discrete exponentials as in

$$I(t) = \sum_{i} \alpha_i \exp(-t/\tau_i), \tag{2}$$

where $I(t)$ is the intensity decay, α_i is the amplitude (preexponential factor), τ_i is the fluorescence lifetime of the ith discrete component, and $\sum\alpha_i = 1.0$. The fractional intensity, f_i, of each decay time is given by

$$f_i = \frac{\alpha_i \tau_i}{\sum_{j} \alpha_j \tau_j} \tag{3}$$

and the mean lifetime is

$$\langle \tau \rangle = \sum_{i} f_i \tau_i. \tag{4}$$

Note on global analyses

To model excited state processes or to unravel heterogeneity in the distribution of fluorophores, experiments under a variety of conditions can be performed. One can change experimental parameters such as excitation and emission wavelengths, pH, quencher concentration, timescale, temperature, orientation of excitation, and emission polarizers. Finally, a multi-dimensional fluorescence decay surface is obtained. From the separate analyses of the individual decay traces, a model can be deduced. The appropriateness of the model is checked by verifying the consistency of the parameter values obtained from each decay curve analysis. However, the parameter estimates resulting from the various single decay curve analyses may suffer from a large uncertainty so that the model building becomes difficult. It has to be realized that many parameters appear in a nonlinear way in the model function and that in most cases the functions within the model are nonorthogonal. It has been suggested to perform a simultaneous analysis of related decay traces, i.e., of the fluorescence decay surface, by linking the common parameters. The merits of this global analysis approach have been emphasized and used broadly within the scientific community (34). Global analysis of fluorescence lifetime data can be used to obtain an accurate fit of multi-exponential fluorescence decays. Global analysis algorithms simultaneously fit multiple measurements acquired under different experimental conditions to achieve higher accuracy (35).

In our studies, the experimental parameter that changes was the preillumination time of the sample, before acquiring the fluorescence decays.

Analysis of denaturation curves

The temperature values at the midpoint of the denaturation curve (T_m where formally 50% of the protein molecules are native and 50% are unfolded) were determined assuming that during transitions two distinct and populated states were present, the native (N) and the unfolded state (U) (8). The observed value of the spectroscopic signal, y, at any point will be $y = y_N f_N + y_U f_U$, where y_N and y_U are the values of y characteristic of the native and unfolded states, respectively, under the conditions where y is being measured. $f_N + f_U = 1$, with f_N and f_U representing the fraction of protein in the native and unfolded conformations. The equilibrium constant, K, and the free energy change, ΔG, can be calculated using $K = (y_N - y)/(y_N - y_U)$, and $\Delta G = -RT\ln K$, where R is the gas constant and T the absolute temperature. T_m values were calculated from a plot of ΔG versus temperature to $\Delta G = 0$.

RESULTS

Extinction coefficient of HRPA2 and hematin

The extinction coefficients of HRPA2 and of hematin from 250 nm to 700 nm are displayed in Fig. 2. In native HRPA2

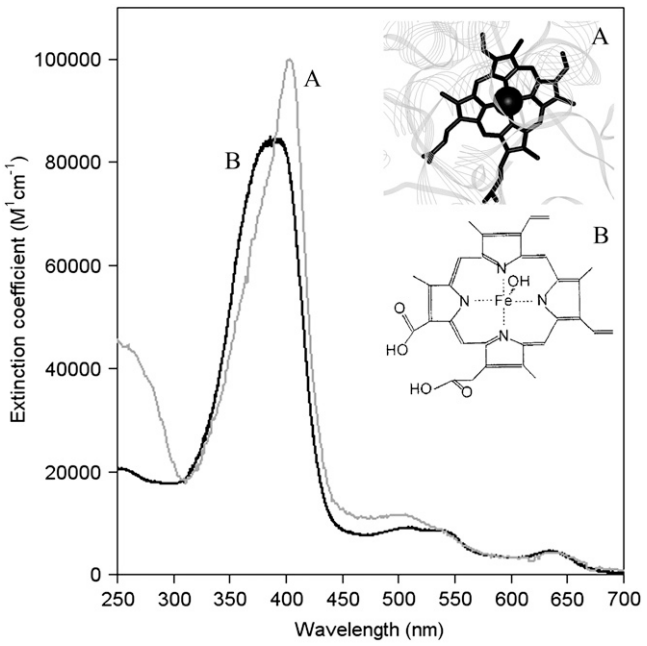

FIGURE 2 Absorption spectra of hematin (*solid curve*) and native HRPA2 (*shaded curve*). Insets show the heme group in peroxidase (*A*) and the hematin molecule (*B*). The hematin extinction coefficients were taken from Du et al. (32). In native HRPA2 the absorption below 300 nm is mainly due to aromatic amino acids and cystines. The peaks around 403 nm and above 475 nm are only due to heme absorption.

the absorption below 300 nm is mainly due to aromatic amino acids and cystines. The peaks around 400 nm and above 475 nm are only due to heme absorption.

Photosensitivity of the tryptophan fluorescence quantum yield

The illumination time-dependent fluorescence intensity of horseradish at 350 nm upon illumination with 296-nm light is shown in Fig. 3 *A*. In the first 20,000 s (5.5 h) a very rapid increase in the number of counts per second can be observed, followed by a short plateau. Afterward, the fluorescence quantum yield was observed to drop upon further illumination of the peroxidase sample. The HRPA2 fluorescence emission observed stems from the single tryptophan residue as excitation light was selected to 296 nm, a wavelength at which Tyr and Phe residues are not excited. After fitting the curve displayed in Fig. 3 *A* to a biexponential function like the one described by Eq. 1, as described in Materials and Methods, where $IF(t)$ is the intensity of the fluorescence measured at time, t, k_i and k_d the rate constants for the increase and decrease of the fluorescence intensity, respectively, and C_i ($i = 1$, 2, or 3) are constants, the values of k_i and k_d are 0.324 h^{-1} and 0.017 h^{-1}, respectively. The physical interpretation of Eq. 1 indicates that irradiation of tryptophan induces two first order reactions, i.e., involving only one enzyme molecule.

Before irradiation, an excitation spectrum (emission at 350 nm) of fresh peroxidase was recorded. Afterward, excitation spectra were recorded after different times of irradiation (22 min, 44 min, 76 min, 116 min, 6 h and 16 h, emission at 350 nm), as displayed in Fig. 3 *B*. It can be observed that an increase in the fluorescence intensity in Fig. 3 *A* is correlated with an increase in the excitation fluorescence intensity displayed in Fig. 3 *B*. Moreover it can be observed that the excitation spectra become increasingly blue shifted the longer the irradiation time (Fig. 3 *B*). Interestingly, when observing the ratio between the normalized excitation spectra (Fig. 3 *C*), being the ratios defined as the intensity of each excitation spectrum divided by the excitation spectrum at time zero, it can be seen that illumination of the peroxidase sample at 296 nm induces spectral changes between 250 and 270 nm, where both Tyr and Trp absorb and fluoresce at 350 nm (Phe does not fluoresce at 350 nm) and above 290 nm, where only Trp absorbs. No spectral changes were observed from ~278 to 290 mn.

Activity and Reinheitzahl value changes in HRPA2 on UV-light irradiation

In peroxidases the catalytic activity is dependent on the presence and correct conformation of the heme group and the residues forming the catalytic pocket. Conformational changes on the protein likely affect enzyme activity. Fig. 4 *A* shows the change of enzyme activity upon different UV illumination times compared to a nonilluminated HRPA2 sample. The change of the Reinheitzahl value (R_z), defined by the ratio between the Soret band absorbance and the absorbance at 280 nm, upon different UV illumination times compared to a nonilluminated HRPA2 sample is also displayed. Activity decays exponentially with a rate constant, k_{act}, 0.00377 min^{-1} (0.23 h^{-1}) for the irradiated sample and 0.00042 min^{-1} (0.03 h^{-1}) for the dark control. Fitting to a double exponential model did not improve the quality of the fit (no improvement on χ^2 and larger errors associated with the fitted parameters). After 16 h of UV illumination the enzyme displayed 2% of its initial activity, whereas the nonirradiated enzyme displayed 65% of its initial activity. The activity of the enzyme when the intensity of the 350-nm emission is at its maximum (~6 h of irradiation at 296 nm) is ~30% of the initial, whereas the nonirradiated sample maintained 92% of the initial activity value after the same period of time.

The R_z value of peroxidase dropped significantly upon UV excitation. After 6 h and 16 h of UV illumination, the R_z value was reduced from ~3.70 to 1.18 and 1.16, respectively, 31% of the initial value. Over the same period, the R_z values of the nonilluminated sample decreased from 3.39 to 2.96 and 2.94 after 6 h and 16 h at room temperature, 87% of the initial value. The R_z values as a function of illumination time could be described by a single exponential decay with rate constant k_{Rz} of 0.0038 min^{-1} (0.23 h^{-1}). Apparently the

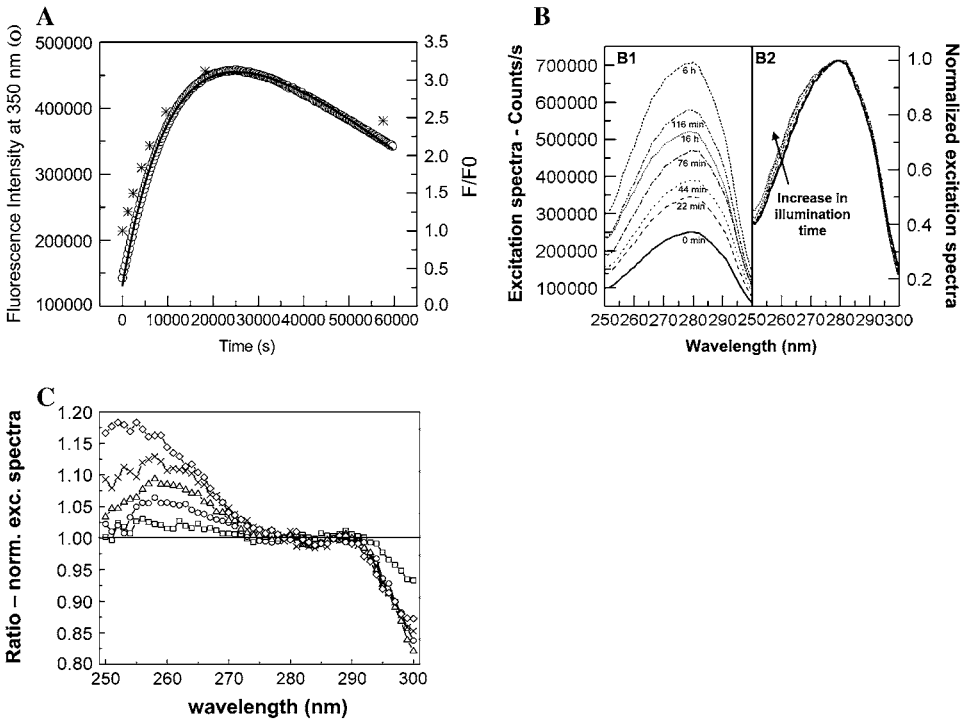

FIGURE 3 (*A*) Tryptophan fluorescence emission intensity of HRPA2 collected at 350 nm as a function of 296-nm irradiation time at 20°C. The line represents the best fit of the bi-exponential function in Eq. 1 to the experimental points. Fit parameters are $k_i = 9 \times 10^{-5}$ s^{-1} (0.324 h^{-1}) and $k_d = 4.8 \times 10^{-6}$ s^{-1} (0.017 h^{-1}) and $r^2 = 0.99862$. The asterisk indicates the ratio of fluorescence increase (F/F_0). (*B*) Effect of irradiation time on excitation spectra (*B1*) and normalized excitation spectra (*B2*) of HRPA2. (*Solid curve*) 0 min; (*long dash curve*) 22 min; (*larger dot curve*) 44 min; (*dash-dot-dash curve*) 76 min; (*dash-dot-dot curve*) 116 min; (*short dash curve*) 6 h; and (*smaller dot curve*) 16 h. The excitation spectra were acquired setting emission at 350 nm. (*C*) Ratio between the normalized spectra displayed in *B2* for different irradiation times (□) 22 min; (○) 76 min; (△) 184 min; (×) 6 h; and (◇) 16 h and the spectrum for nonirradiated HRPA2.

process is faster for the nonirradiated control sample with a rate constant $k_{Rz,}$ 0.0065 min^{-1} (0.39 h^{-1}). Fitting to a double exponential model did not improve the quality of the fit. The data point for the R_z value observed after 6 h of illumination was more than 10 standard deviations from the model obtained by fitting to the rest of the data points and was thus not considered.

Absorbance spectral changes in HRPA2 on UV-light irradiation

Spectral properties of the HRPA2 heme group as a function of irradiation time are presented in Fig. 4 *B*. Increasing irradiation time at 296 nm lead to a decrease of the Soret absorption band as well as the disappearance of the charge transfer transitions (CT1, 498 nm; CT2, 643 nm) characteristic of a pentacoordinate state of the iron.

UV irradiation-induced changes in secondary structure of HRPA2

Complementary analysis of protein conformational alterations was investigated by circular dichroism (CD) spectroscopy. Thermal stability of 5 μM HRPA2 samples irradiated with light at 296 nm for 6 and 16 h were investigated. The respective control measurements were performed. Temperature

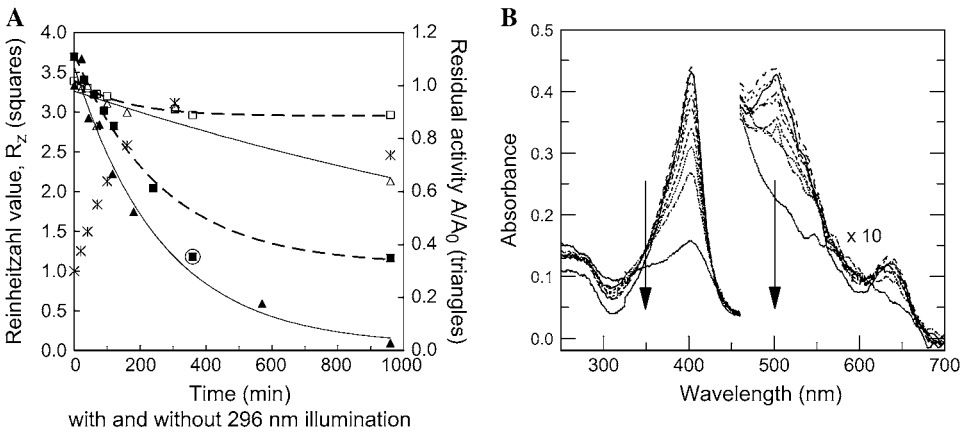

FIGURE 4 (*A*) Residual activity (A/A_o, *triangles*) and R_z (*squares*) of HRPA2 as a function of 296-nm illumination time (*solid triangles* and *squares*) and of a nonilluminated control sample (*open triangles* and *squares*). The solid and dashed lines correspond to a first order exponential decay fit of residual activity and R_z value, respectively. Fit parameters are $k_{act} = 0.00377$ min^{-1} (0.23 h^{-1}) for the irradiated sample and $k_{act} = 0.00042$ min^{-1} (0.03 h^{-1}) for the control sample; $k_{Rz} = 0.0038$ min^{-1} (0.23 h^{-1}) for the irradiated sample and $k_{Rz} = 0.0063$ min^{-1} (0.38 h^{-1}) for the control sample. The asterisk corresponds to the ratio of fluorescence increase (F/F_0) as a function of 296-nm illumination time as displayed in Fig. 3 *A*. (*B*) Dependence of HRPA2 optical absorption on 296-nm irradiation time. The arrow indicates increasing irradiation time.

dependence of the ellipticity at 223 nm of native HRPA2 and samples irradiated for different periods of time are shown in Fig. 5. Data reveal that the longer the irradiation period the lower the melting temperature, T_m, of HRPA2 at pH 4, as displayed in Table 1. After 6-h UV illumination, the T_m of the protein dropped 2.25 K and its ellipticity at 295 K dropped from -16 degcm^{2}dmol^{-1} to -11 degcm^{2}dmol^{-1}. After a 16-h UV illumination, the protein still showed the presence of secondary structure elements (ellipticity had decreased from -16 degcm^{2}dmol^{-1} to a residual value of -8×10^{-3} degcm^{2}dmol^{-1} at 295 K) although no transition was detected in the temperature scans. Fig. 5 clearly shows that irradiation leads to protein denaturation. Concerning the nonirradiated sample, a 16-h period waiting time at room temperature after the sample had been freshly prepared lead to a decrease in the T_m value of 1.4 K (Table 1). No significant helical loss monitored by CD was observed (data not shown).

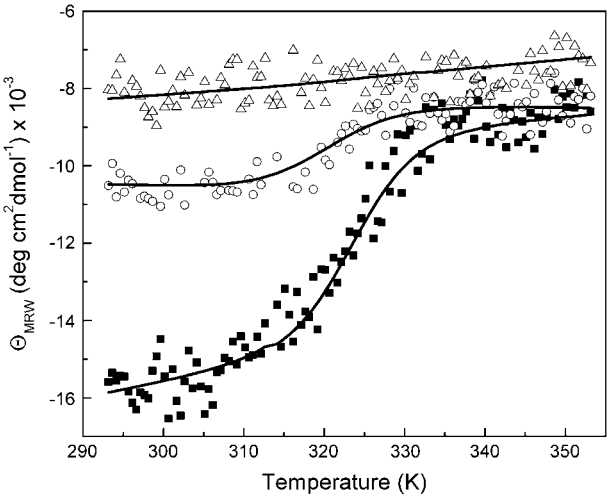

FIGURE 5 Temperature dependence of the ellipticity value at 223 nm of HRPA2: freshly prepared (*squares*), after 6-h irradiation with 296-nm light (*circles*), and after 16-h irradiation with 296-nm light (*triangles*).

Time-resolved lifetime measurements

Streak camera data (Fig. 6 *A*) were analyzed with MATLAB (The MathWorks, Natick, MA) software developed at our department. The two fastest picosecond fluorescence emission lifetimes of HRPA2 observed after different 280-nm illumination times were recovered by global analysis: 100.0 ± 1.4 ps and 746.4 ± 33.5 ps. The third nanosecond lasting fluorescence emission lifetime could not be observed due to the 1.8-ns temporal window seen by our ultrafast streak camera detector. The preexponential factors of the two lifetimes are plotted in Fig. 6 *B* and displayed in Table 2. The shortest lifetime component is dominating the decay in the observation time window at all 280 illumination times. However, as illumination time increases, the longer lifetime component increases from 0.07 ± 0.03 at the beginning of the illumination to a plateau of 0.18 ± 0.02 after 2 h of illumination, as displayed in Fig. 6 *B*. The mean lifetime increased in the same period from 332 ps to plateau at 501 ps, as displayed in Fig. 6 *C*.

TABLE 1 Enzyme residual activity (% of remaining activity compared with initial activity, $A(t)/A_0$), R_z (R_z after time, t, compared to the initial R_z, i.e., $R_z(t)/R_z(t_0) \times 100$) and melting temperature (T_m) values determined by CD spectroscopy after 6 h and 16 h in a nonirradiated (Non-Irr) and an irradiated (Irr) sample with 296-nm UV light

	$A(t)/A_0$ (%)		$R_z(t)/R_z(t_0)$ (%)		ΔT_m (K)	
Time	Non-Irr	Irr	Non-Irr	Irr	Non-Irr	Irr
6 h	92	30*	87	32	n.d.	2.25
16 h	64	3	87	31	1.4	n.t.

The values are compared to the enzyme's initial values immediately after the solution has been prepared.
n.d., nondetermined; n.t. no transition detected.
*From curve interpolation.

A comparison of the data obtained by continuously illuminating the HRP solution with 280-nm and 290-nm light is displayed in Table 3.

Fluorescence and absorption spectra changes induced by illumination at 403 nm

Excitation of HRPA2 at 403 nm, where the heme group displayed maximum absorbance, also had an effect on the protein's Trp fluorescence. During the experiment where HRPA2 was continuously illuminated at 403 nm, the protein's Trp fluorescence emission intensity at 350 nm upon 296-nm excitation was measured at different times over a period of more than 30 h. The emission intensity was observed to increase more the longer the illumination time at 403 nm, reaching approximately twice the initial Trp fluorescence intensity after 30 h of exposure to the 403-nm light, as displayed in Fig. 7 *A*.

Furthermore, 403-nm continuous illumination changed the absorption spectrum of a HRPA2 solution, as displayed in Fig. 7 *B*. After 26 h of 403-nm illumination the distinct Soret band peak changes shape, intensity, and absorption peak. The CT1 transition around 500 nm is affected as well.

DISCUSSION

The results presented in this study do show that prolonged UV illumination of horseradish peroxidase affects its catalytic activity, structural thermal stability, R_z, heme absorption bands, fluorescence quantum yield, fluorescence excitation and emission spectra, fluorescence lifetime distribution, and fluorescence mean lifetime. UV illumination aimed at excitation of the protein's aromatic pool at 280 nm and 296 nm or specifically excitation of its prosthetic group, ferriprotoporphyrin IX (Fe-PPIX), at 403 nm.

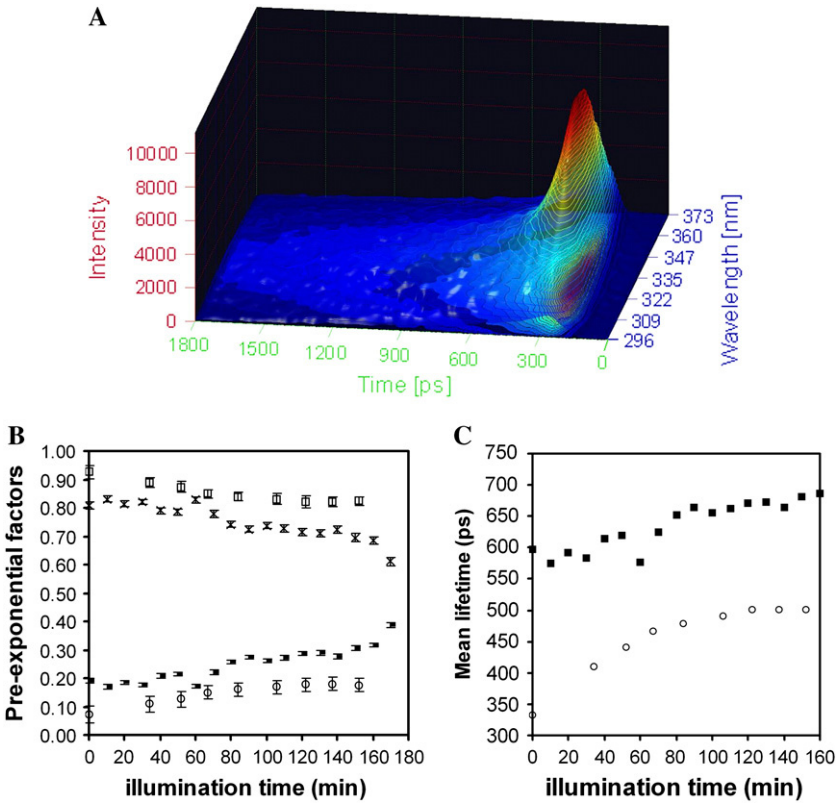

FIGURE 6 (*A*) Three-dimensional representation of a temporally and spectrally resolved streak camera image of the fluorescence emission decay of HRPA2 upon 280-nm excitation. (*B*) Distribution of the preexponential factors associated with the two fastest lifetime components of HRPA2 (100 ± 1 ps, *open squares*; 746 ± 34 ps, *open circles*) as a function of 280-nm illumination time; Distribution of the preexponential factors associated with the two fastest lifetime components of HRPA2 (83 ± 0.8 ps, *cross* and 819 ± 37 ps *horizontal bar*) as a function of 290-nm illumination time. See also Table 3; (*C*) Mean fluorescence lifetime of HRPA2 as a function of 280-nm (*open circles*) and 290-nm (*solid squares*) illumination times.

Fluorescence quantum yield

The results show that excitation of the protein at all mentioned wavelengths lead to an increase in the fluorescence quantum yield of the protein, observation correlated with loss of absorption of the heme group (Figs. 4 *B* and 7 *B*). Fluorescence intensity of the single tryptophan residue of HRPA2 in its native state is highly quenched because of the presence of an adjacent prosthetic group, Fe-PPIX. The efficiency of energy transfer (E) between the Trp donor and the heme acceptor is almost maximum, e.g., in horseradish peroxidase (HRPC) E is 0.93 (10) and in soybean peroxidase E is 0.97 (7). Tryptophan quantum yield is known to be ~0.001 in classic plant peroxidases due to energy transfer to the heme group. This value increases 20 and 10 times for apoproteins of horseradish peroxidase C and soybean peroxidase, respectively (7,9). However, as displayed in Figs. 3 *A* and 7 *A*, excitation of horseradish peroxidase at 296 nm and 403 nm increased its fluorescence quantum yield. The increase might be due to light-induced separation of the Trp residue from the quencher heme group and/or photoinduced chemical changes in the prosthetic group of HRPA2. The first hypothesis is supported by the work done by Gryczynski and Bucci (36) on another heme-containing protein, horse heart myoglobin, and by the work of Grotjohann et al. (27) on photoinactivation of a plant catalase, also a heme protein. Grotjohann et al. showed that blue light excitation of catalase would induce heme dissociation and heme photochemistry. Grotjohann et al. also report that the velocity of heme destruction is lower than the rate of enzyme photoinactivation, suggesting that other photoinduced reactions lead to enzyme inactivation. Gryczynski and Bucci observed that the steady-state fluorescence emission intensity was reversibly increased with decreasing pH, almost doubling at pH 4.5, and was correlated with an increase in heme dissociability at lower pH, consistent with the titration of the proximal and distal histidines inside the heme pocket. Their analyses revealed the presence of three species originating

TABLE 2 Preexponential factors associated to the fluorescence lifetimes recovered from the fluorescence decay of HRPA2, detected with streak camera after 280-nm illumination

	Preexponential factors	
Illumination time (min)	Short lifetime (100 ± 1 ps)	Long lifetime (746 ± 34 ps)
0	0.93 ± 0.02	0.07 ± 0.03
34	0.89 ± 0.02	0.11 ± 0.03
52	0.87 ± 0.02	0.13 ± 0.03
67	0.85 ± 0.02	0.15 ± 0.02
84	0.84 ± 0.02	0.16 ± 0.02
106	0.83 ± 0.02	0.17 ± 0.02
122	0.82 ± 0.02	0.18 ± 0.02
137	0.82 ± 0.02	0.18 ± 0.02
152	0.82 ± 0.02	0.18 ± 0.02

TABLE 3 Comparison of the data obtained by continuously illuminating the HRP solution with a 280-nm and 290-nm laser beam. τ_{short}: short lifetime; τ_{long}: long lifetime; α: preexponential factor associated to each lifetime

Excitation	τ_{short}	τ_{long}	α_{short}		α_{long}		$\langle\tau\rangle$	
			Start	End	Start	End	Start	End
280 nm	100 ± 1 ps	746 ± 34 ps	0.93 ± 0.02	0.82 ± 0.02	0.07 ± 0.03	0.18 ± 0.02	332 ps	501 ps
290 nm	83 ± 0.8 ps	819 ± 37 ps	0.81 ± 0.01	0.61 ± 0.02	0.19 ± 0.01	0.39 ± 0.01	597 ps	717 ps

$\langle\tau\rangle$ is the fluorescence mean lifetime.

from heme-protein interactions with three distinct fluorescence lifetimes: the native form of crystalline protein (30–114 ps), the conformation with disordered hemes (240–1400 ps), and the reversibly dissociated heme-free myoglobin (3100–5100 ps).

This work has been done at pH 4. Acidic pH values will favor the protonation of the distal and proximal His residues in HRPA2, which pKa values have been reported to be ~2.5 for the distal His (1) and below 3 for the proximal His (37), for horseradish peroxidase C. Wolff et al. recently estimated, using NMR, the pK_a of the His-32 that binds heme in the protein $HasA_{SM}$ as being below 4.8 (38). These pK_a values are considerably lower than the pK_a of His when in the model tripeptide Gly-His-Gly ($pK_{model} = 6.4$) (39). Once protonated, the positively charged His will electrostatically repulse the nearby positively charged heme group and catalytic Arg, which is positively charged at acidic pHs (Fig. 1 *B*). Therefore, acidic pH values will induce conformational changes in the active side pocket of peroxidases that might induce heme release (40). Low pH is actually used to induce release of heme from the protein to create the apoprotein (41). Ejection of the heme group has been reported to lead to an irreversible thermal unfolding of HRPA2 and HRPA1 at pH 4, whereas at pH 7 and 10 refolding was observed (8) since the protein recaptures the heme group upon cooling. This is correlated with the electrostatic repulsion between the heme group and the heme moiety at acidic pH values. The presence of positively charged groups renders the pK_a value of both the distal and proximal His considerably lower than its pK_{model} since once neutral, there will be no electrostatic repulsions between the His and the positively charged groups. Also, since the distal His will the hydrogen-bond acceptor upon binding H_2O_2, it will be a better acceptor if neutral. These are two likely reasons that contribute to the low pK_a value of proximal and distal His observed in peroxidases.

An increase in fluorescence emission intensity upon UV excitation of the single Trp residue in other proteins, like cutinase, has been observed by Weisenborn et al. (42), Prompers et al. (20), and Neves-Petersen et al. (21). The reason for the observed increase in fluorescence emission intensity was the disruption of the disulphide bridge, an excellent protein fluorescence quencher, located near the Trp residue upon Trp UV excitation (20,21,23). The study reported in this work points at a similar possible mechanism explaining the increase in fluorescence intensity of HRPA2 upon UV illumination: putative light-induced dissociation and/or photoinduced damage of the strong fluorescence quencher in horseradish peroxidase, the prosthetic group ferriprotoporphyrin IX, and the heme moiety. In the Protein Data Bank structure of the highly homologous *Arabidopsis thaliana* peroxidase A2 (Fig. 1 *A*), this group is located within 8 Å (closest distance) from the Trp residue. The closer a quencher is from the fluorescence donor and the higher its extinction coefficient, the stronger the quenching will be. The disulphide bridges in HRPA2 are located farther away from the Trp residue, which means that in terms of distance the prosthetic group is a better fluorescence quencher.

Furthermore, compared to disulphide bridges, the prosthetic ferriprotoporphyrin IX group has a much larger extinction coefficient in the wavelength range where Trp emits (43). Therefore it is the prosthetic group in peroxidases

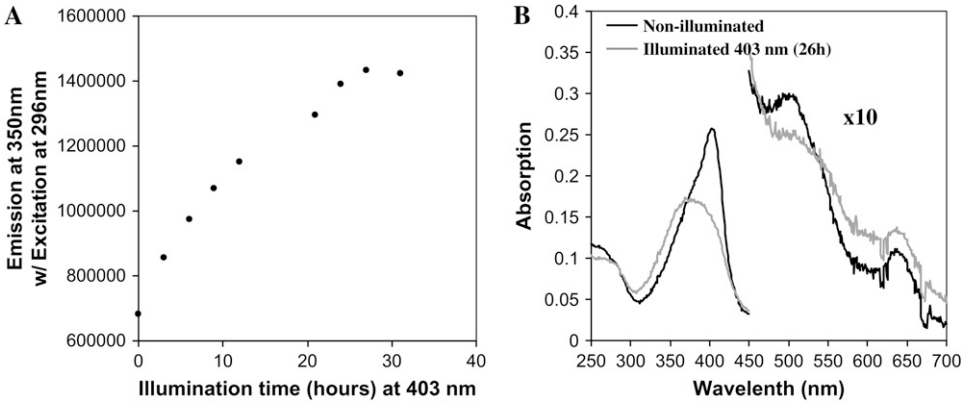

FIGURE 7 (*A*) Effect of 403-nm illumination time (heme excitation) on the protein's fluorescence emission intensity at 350 nm obtained upon 296-nm excitation. Fluorescence emission spectra were acquired after 0, 3, 6, 9, 12, 21, 24, 27, and 31 h of illumination at 403 nm. (*B*) Absorption spectra of native HRPA2 (*solid line*) and of HRPA2 illuminated for 26 h at 403 nm (*shaded line*).

that is mainly responsible for the proteins' fluorescence emission intensity due to its quencher properties. The changes reported here in the absorption spectrum of ferriprotoporphyrin IX group upon UV illumination of horseradish peroxidase (both 296 nm and 403 nm; Figs. 4 *B* and 7 *A*) suggest that the prosthetic group putatively dissociates from the protein and/or suffers photodamage upon UV illumination. Irradiation of Trp in HRPA2 can induce alterations in the protein moiety through electron transfer from triplet states of Trp (^{3}Trp) to suitable acceptors such as cystines (13). The UV light-induced opening of disulphide bridges upon excitation of the protein's aromatic residues was observed for many other proteins, such as hydrolytic enzymes (lipases/esterases, lysozyme), proteases (human plasminogen), alkaline phosphatase, immunoglobulins' Fab fragment, major histocompability complex class I protein (23), and α-lactalbumin (22). Detection of free thiols groups was observed after photoinduced disruption of the disulphide bridges. HRPA2 contains eight cysteine residues involved in four disulphide bridges conserved in all members of the classical plant peroxidases class. The nearest cystine in the *A. thaliana* peroxidase A2 (ATPA2) crystal structure (Fig. 1 *A*) is located ~12 Å from the single Trp residue. Photoinduced disruption of disulphide bridges located as far as 10 Å from the aromatic residue has been reported for α-lactalbumin (22).

Molecular photobleaching

Fig. 3 *A* also shows that prolonged UV illumination (after ~7-h illumination at 296 nm) leads to molecular photobleaching, leading to a decrease in the fluorescence intensity. A possible UV-induced reaction in proteins leads to, e.g., electron transfer, ionization, and radical formation (12–14,25,44–56, S. Klitgaard, M. T. Neves-Petersen, V. Sundström, T. Polivka, A. Yartsev, T. Pascher, and S. B. Petersen, unpublished). These photoinduced reactions lead to photochemical changes of the fluorophores, with concomitant conversion of the indole chromophore into a nonfluorescing group (42). Photobleaching originates from the triplet excited state, which is created from the singlet state (S1) via intersystem crossing.

Protein stability, heme absorption, and Reinheitzahl values

CD data clearly show that prolonged UV irradiation leads to protein denaturation. After 16-h UV illumination no transition is detected in the temperature scans, as displayed in Fig. 5. This observation is correlated with data presented in Fig. 3 *A*, which indicate that after 16 h of UV illumination the protein has already suffered photophysical- and photochemical-induced reactions leading to photobleaching. These reactions will lead to structural damage of proteins that will ultimately impair their activity. As can be seen in Table 1 and Fig. 4 *A*, after 6 h and 16 h of UV illumination the protein's residual activity was 30% and 2%, respectively.

It was also observed in our study that illumination of HRPA2 with 296 nm and 403 nm leads to loss in the Soret absorbance band, as displayed in Figs. 4 *B* and 7 *B*, respectively. The intensity of the visible bands at ~500 nm and 643 nm also decrease with longer irradiation periods of time. Heme release has been reported to be the first event occurring during unfolding of HRPA2 (8). These observations do correlate with the hypothesis that light induces heme dissociation and/or chemical modification of the heme group.

UV illumination has also affected the protein's R_z and its thermal stability. Residual ellipticity was observed after denaturation of horseradish peroxidase (Fig. 5). The observed decrease in the HRPA2 Soret band absorbance upon UV illumination lead to a decrease in the R_z value of the protein and was accompanied by activity loss (Fig. 4). Both R_z and activity values decay exponentially with identical first order decay constants (k_{act} and k_{Rz}), which might indicate that light-induced changes in the heme moiety and the aromatic pool moiety do lead to changes in the structure and therefore in the activity of the protein. Irradiation damage was observed to be immediate. The loss of secondary structural elements upon UV irradiation (Fig. 5) reveals that photophysical and photochemical processes initiated in the Trp residue and probably on the adjacent heme group are damaging the overall structure of HRPA2. The lower melting temperature, T_m, of HRPA2 upon irradiation (Table 1) as well as the decrease in the far-UV ellipticity after 6-h irradiation (Fig. 5) is likely to be caused by light-induced structural changes in the heme environment. The proximal His is covalently bound to the heme iron and responsible for the heme architecture and consequently the enzyme activity (2). Conformation changes in the heme moiety will affect the active site architecture.

Photochemistry, reactive oxygen species

Oxidation of histidine, present in the catalytic center of catalases is perhaps an early event in catalase photoinactivation as it is an oxygen-dependent process (27). Likewise, oxidation of proximal His in HRPA2 might be responsible for the enzyme activity loss and heme spectra alterations. Indirect photooxidation of proteins is known to occur via the formation and subsequent reactions of singlet oxygen. Heme moieties have, in general, the capability to generate reactive oxygen (29). Other amino acid residues in the protein are susceptible to reacting with $^1O_2$, namely excited Trp and Tyr, Met, or Cys, leading to chemical changes of these residues. It is known that *N*-formylkynurenine, a tryptophan photoproduct, can act as an endogenous photosensitizer that can generate singlet oxygen and superoxide. Tyr radicals are also reported to be formed after excitation of Trp residues (49). Trp can transfer energy to Tyr residues via Förster-type singlet energy transfer (57). The process of

HRPA2 photoinactivation is likely to be induced also by formation of $^1O_2$ upon heme excitation and since the heme group is a sensitizer that once in the excited state can undergo intersystem crossing, enter a triplet state, and react with molecular oxygen generating singlet oxygen, one of the most reactive oxygen species.

Both illumination of aromatic residues and of the heme group leads to changes in heme absorption and fluorescence quantum yield of horseradish peroxidase, indicative of heme leaving the molecule and/or photoinduced chemical changes in the heme moiety. Direct illumination of the heme group can induce photochemical reactions such as electron ejection from the porphyrin ring, associated to cation and radical formation, and singlet oxygen formation that can change the conformation of the heme pocket. The excited state aromatic residues in $HRPA_2$ will deliver a great part of their excitation energy to the prosthetic ferriprotoporphyrin IX group, since this is an effective fluorescence quencher. Furthermore, since UV illumination of aromatic residues leads to electron ejection from their side chains (see references above), it is likely that the prosthetic group also acts as an electron acceptor, further destabilizing the heme pocket.

Spectral changes of aromatic residues

As displayed in Fig. 3, *B* and *C*, prolonged UV illumination of $HRPA_2$ lead to spectral shifts in the excitation spectra of the protein. This is indicative of chemical changes suffered by the Trp or other aromatic residues in the protein. Trp has been selectively excited at 296 nm. We can see from Fig. 3 *C* that this lead to a change in the excitation spectra above 292 nm, where Trp absorbs. If Tyr residues were also excited due to Förster-type singlet energy transfer from Trp residues, phenolate anions ($PheO^-$) could have been created. The pKa of the OH group in UV-excited Tyr residues is expected to be around 4 (32), and thus much lower than the pK_a around 10 for ground state tyrosine (39). $PheO^-$ is known to have larger extinction coefficients above 290 and fluorescence emission is centered around 345 nm (11,39). Fig. 3 *C* shows that changes are also observed from 250 nm to 275 nm. No changes are observed from ~275 nm to 290 nm. Since these spectra have been obtained with emission set to 350 nm, the excitation spectra report changes only on Trp and Tyr residues, since Phe do not emit at 350 nm.

Fluorescence lifetime studies

Peroxidases are usually characterized by three fluorescence lifetimes: in HRPA1, pH 7, the three lifetimes are 55 ps, 130 ps, and 1.2 ns (58) and in HRPC the observed lifetimes were 45–76 ps, 1.1–1.5 ns, and 3.9–4.9 ns, depending on pH (10). In this study, with the detection system used (streak camera), we have only observed picosecond lifetime components since the streak camera has a temporal window of 1.8 ns. The longest nanosecond fluorescent lifetime component was not observed. In our study we are interested in following changes in the short lifetime components. The shortest picosecond lifetime components are known to be associated to the heme group here. Changes in the heme moiety will most likely induce changes in the fluorescence lifetime distribution.

As can be seen from Fig. 6, *B* and *C*, and Table 2, the two fastest relaxation pathways of horseradish peroxidase are characterized by lifetimes of 100 ± 1 ps and 746 ± 34 ps (when using 280-nm excitation), respectively, and 83 ± 0.8 ps and 819 ± 37 ps (when using 290-nm excitation), respectively. The observed change in the preexponential factors associated with each of the above mentioned lifetimes, as a function of UV illumination time, leads to an increase in the protein's mean lifetime. This observation supports the hypothesis that UV light induced dissociation of the strong protein fluorescence quencher group, the ferriprotoporphyrin IX group, and/or chemical changes in the heme moiety.

The effect of preillumination of HRP at 403 nm, where heme absorbs, on the dynamics of HRP fluorescence emission, upon 280 nm and 290 nm excitation, has also been studied (data not shown). Preillumination of the heme group leads to an increase of the fluorescence mean lifetime of horseradish peroxidase.

CONCLUDING REMARKS

The study of the interaction between light and biomolecules will give us insight into the fantastic work of energy exchange in a molecule. From such studies, the role of energy donors and acceptors will be clearer, as well as which energies are involved, which photoinduced reactions are triggered as well as the timescales of each light-driven step. The ultimate goal will be to control energy transfer in proteins and eventually reaction mechanisms.

The authors declare that they have no competing financial interests.

M.T.N.-P. acknowledges the support from Novi Invest and Licfond and from the Danish Research Agency, Novo Nordisk A/S, Novozymes A/S.

REFERENCES

1. Dunford, H. B. 1999. Heme Peroxidases. Wiley-VCH, New York.
2. Veitch, N. C., and A. T. Smith. 2001. Horseradish peroxidase. *Adv. Inorg. Chem.* 51:107–162.
3. Mauro, J. M., L. A. Fishel, J. T. Hazzard, T. E. Meyer, G. Tollin, M. A. Cusanovich, and J. Kraut. 1988. Tryptophan-191—phenylalanine, a proximal-side mutation in yeast cytochrome *c* peroxidase that strongly affects the kinetics of ferrocytochrome *c* oxidation. *Biochemistry.* 27:6243–6256.
4. Sivaraja, M., D. B. Goodin, M. Smith, and B. M. Hoffman. 1989. Identification by ENDOR of Trp191 as the free-radical site in cytochrome *c* peroxidase compound ES. *Science.* 245:738–740.
5. Brunet, J. E., G. A. Gonzalez, and C. P. Sotomayor. 1983. Intramolecular tryptophan heme energy transfer in horseradish peroxidase. *Photochem. Photobiol.* 38:253–254.

6. Pappa, H. S., and A. E. G. Cass. 1993. A step towards understanding the folding mechanism of horseradish peroxidase. Tryptophan fluorescence and circular dichroism equilibrium studies. *Eur. J. Biochem.* 212: 227–235.
7. Kamal, J. K., and D. V. Behere. 2001. Steady-state and picosecond time-resolved fluorescence studies on native and apo seed coat soybean peroxidase. *Biochem. Biophys. Res. Commun.* 289:427–433.
8. Carvalho, A. S., E. P. Melo, B. S. Ferreira, M. T. Neves-Petersen, S. B. Petersen, and M. R. Aires-Barros. 2003. Heme and pH-dependent stability of an anionic horseradish peroxidase. *Arch. Biochem. Biophys.* 415: 257–267.
9. Das, T., and S. Mazumdar. 1995. Conformational substates of apoprotein of horseradish peroxidase in aqueous solution: a fluorescence dynamics study. *J. Phys. Chem.* 99:13283–13290.
10. Das, T., and S. Mazumdar. 1995. pH-induced conformational perturbation in horseradish peroxidase. Picosecond tryptophan fluorescence studies on native and cyanide-modified enzymes. *Eur. J. Biochem.* 227:823–828.
11. Lakowicz, J. R. 1999. Principles of Fluorescence Spectroscopy, 2nd ed. Kluwer Academic/Plenum Publishers, New York.
12. Bent, D. V., and E. Hayon. 1975. Excited state chemistry of aromatic amino acids and related peptides. I. Tyrosine. *J. Am. Chem. Soc.* 97:2599–2606.
13. Bent, D. V., and E. Hayon. 1975. Excited state chemistry of aromatic amino acids and related peptides. III. Tryptophan. *J. Am. Chem. Soc.* 97:2612–2619.
14. Creed, D. 1983. The photophysics and photochemistry of the near-UV absorbing amino acids-II. Tyrosine and its simple derivatives. *Photochem. Photobiol.* 39:563–575.
15. Augenstein, L., and P. Riley. 1964. The inactivation of enzymes by ultraviolet light, IV: the nature and involvement of cystine disruption. *Photochem. Photobiol.* 3:353–367.
16. Igelman, J. M., T. C. Rotte, E. Schecter, and D. J. Blaney. 1965. Exposure of enzymes to laser radiation. *Ann. N. Y. Acad. Sci.* 122: 790–801.
17. Berns, M. W., S. I. Matsui, R. S. Olson, and D. E. Rounds. 1970. Enzyme inactivation with ultraviolet laser energy (2650 Angstroms). *Science.* 169:1215–1217.
18. Saha, A. 1997. Photo-induced inactivation of dihydroorotate dihydrogenase in dilute aqueous solution. *Int. J. Radiat. Biol.* 72:55–61.
19. Vladimirov, Y. A., D. I. Roshchupkin, and E. E. Fesenko. 1970. Photochemical reactions in amino acid residues and inactivation of enzymes during U.V.-irradiation. A review. *Photochem. Photobiol.* 11:227–246.
20. Prompers, J. J., C. W. Hilbers, and H. A. M. Pepermans. 1999. Tryptophan mediated photoreduction of disulfide bond causes unusual fluorescence behaviour of Fusarium solini pisi cutinase. *FEBS Lett.* 456:409–416.
21. Neves-Petersen, M. T., Z. Gryczynski, J. Lakowicz, P. Fojan, S. Pedersen, E. Petersen, and S. B. Petersen. 2002. High probability of disrupting a disulphide bridge mediated by an endogenous excited tryptophan residue. *Protein Sci.* 11:588–600.
22. Vanhooren, A., B. Devreese, K. Vanhee, J. van Beumen, and I. Hanssens. 2002. Photoexcitation of tryptophan groups induces reduction of two disulfide bonds in goat α-lactalbumin. *Biochemistry.* 41:11035–11043.
23. Neves-Petersen, M. T., T. Snabe, S. Klitgaard, M. Duroux, and S. B. petersen. 2006. Photonic biosensors: UV light induced molecular switch allows sterically oriented immobilisation of biomolecules and the creation of protein nanoarrays. *Protein Sci.* 11:343–351.
24. Aeschbach, R., R. Amado, and H. Neukom. 1976. Formation of dityrosine cross-links in proteins by oxidation of tyrosine residues. *Biochim. Biophys. Acta.* 439:292–301.
25. Bhattacharya, D., S. Basu, and P. C. Mandal. 2000. UV radiation effects on flavocytochrome b2 in dilute aqueous solution. *J. Photochem. Photobiol. B.* 59:54–63.
26. Greenbaum, L., C. Rothmann, R. Lavie, and Z. Malik. 2000. Green fluorescent protein photobleaching: a model for protein damage by endogenous and exogenous singlet oxygen. *Biol. Chem.* 381:1251–1258.
27. Grotjohann, N., A. Janning, and R. Eising. 1997. In vitro photoinactivation of catalase isoforms from cotyledons of sunflower (Helianthus annuus L.). *Arch. Biochem. Biophys.* 346:208–218.
28. Aubailly, M., J. Haigle, A. Giordani, P. Morliere, and R. Santus. 2000. UV photolysis of catalase revisited: a spectral study of photolytic intermediates. *J. Photochem. Photobiol. B.* 56:61–67.
29. Aft, R. L., and G. C. Mueller. 1984. Hemin-mediated oxidative degradation of proteins. *J. Biol. Chem.* 259:301–305.
30. Shannon, L. M., E. Kay, and J. Y. Lew. 1966. Peroxidase isozymes from horseradish roots. I. Isolation and physical properties. *J. Biol. Chem.* 241:2166–2172.
31. Hiner, A. N., J. Hernández-Ruíz, M. B. Arnao, F. García-Cánovas, and M. Acosta. 1996. A comparative study of the purity, enzyme activity, and inactivation by hydrogen peroxide of commercially available horseradish peroxidase isoenzymes A and C. *Biotechnol. Bioeng.* 50:655–662.
32. Strickland, E. H., E. Kay, L. M. Shannon, and J. Horwitz. 1968. Peroxidase isoenzymes from horseradish roots. 3. Circular dichroism of isoenzymes and apoisoenzymes. *J. Biol. Chem.* 243:3560–3565.
33. Du, H., R. A. Fuh, J. Li, A. Corkan, and J. S. Lindsey. 1998. PhotochemCAD: A computer-aided design and research tool in photochemistry. *Photochem. Photobiol.* 68:141–142.
34. Janssens, L. D., N. Boens, M. Ameloot, and F. C. De Schryver. 1990. A systematic study of the global analysis of multlexponential fluorescence decay surfaces using reference convolution. *J. Phys. Chem.* 94:3564–3576.
35. Verveer, P. J., A. Squire, and P. I. Bastiaens. 2000. Global analysis of fluorescence lifetime imaging microscopy data. *Biophys J.* 78:2127–2137.
36. Gryczynski, Z., and E. Bucci. 1998. Time resolved emissions in the picosecond range of single tryptophan recombinant myoglobins reveal the presence of long range heme protein interactions. *Biophys. Chem.* 74:187–196.
37. Ascenzi, P., M. Brunori, M. Coletta, and A. Desideri. 1989. pH effects on the haem iron co-ordination state in the nitric oxide and deoxy derivatives of ferrous horseradish peroxidase and cytochrome *c* peroxidase. *Biochem. J.* 258:473–478.
38. Wolff, N., C. Deniau, S. Letoffe, C. Simenel, V. Kumar, I. Stojiljkovic, C. Wandersman, M. Delepierre, and A. Lecroisey. 2002. Histidine pK_a shifts and changes of tautomeric states induced by the binding of gallium-protoporphyrin IX in the hemophore $HasA_{SM}$. *Protein Sci.* 11:757–765.
39. Creighton, T. E. 1993. Proteins: Structure and Molecular Properties, 2nd ed. W. H. Freeman & Company, New York.
40. Smith, A., and R. T. Hunt. 1990. Hemopexin joins transferrin as representative members of a distinct class of receptor-mediated endocytic transport systems. *Eur. J. Cell Biol.* 53:234–245.
41. Schulz, H., H. Hennecke, and L. Thöny-Meyer. 1998. Prototype of a heme chaperone essential for cytochrome *c* maturation. *Science.* 281:1197–1200.
42. Weisenborn, P. C. M., H. Meder, M. R. Egmond, T. J. W. G. Visser, and A. van Hoek. 1996. Photophysics of the single tryptophan residue in Fusarium solani Cutinase: evidence for the occurrence of conformational substates with unusual fluorescence behaviour. *Biophys. Chem.* 58:281–288.
43. Klitgaard, S., M. T. Neves-Petersen, and S. B. Petersen. 2006. Quenchers induce wavelength dependence on protein fluorescence lifetimes. *J. Fluoresc.* 16:595–609.
44. Grossweiner, L. I., G. W. Swenson, and E. F. Zwicker. 1963. Photochemical generation of the hydrated electron. *Science.* 141:805–806.
45. Bent, D. V., and E. Hayon. 1975. Excited state chemistry of aromatic amino acids and related peptides. II. Phenylalanine. *J. Am. Chem. Soc.* 97:2606–2612.

46. Hoffman, M. Z., and E. Hayon. 1972. One-electron reduction of the disulfide linkage in aqueous solution. Formation, protonation, and decay kinetics of the $RSSR^-$ radical. *J. Am. Chem. Soc.* 94:7950–7957.

47. Robbins, R. J., G. R. Fleming, G. S. Beddard, G. W. Robinson, P. J. Thistlethwaite, and G. J. Woolfe. 1980. Photophysics of aqueous tryptophan: pH and temperature effects. *J. Am. Chem. Soc.* 102:6271–6279.

48. Mialocq, J. C., E. Amouyal, A. Barnas, and D. Grand. 1982. Picosecond laser photolysis of aqueous indole and tryptophan. *J. Phys. Chem.* 86:3173–3177.

49. Grossweiner, L. I. 1984. Photochemistry of proteins: a review. *Curr. Eye Res.* 3:137–143.

50. Kandori, H., R. F. Borkman, and K. Yoshihara. 1993. Picosecond transient absorption of aqueous tryptophan. *J. Phys. Chem.* 97:9664–9667.

51. Stevenson, K. L., G. A. Papadantonakis, and P. R. LeBreton. 2000. Nanosecond UV laser photoionization of aqueous tryptophan: temperature dependence of quantum yield, mechanism, and kinetics of hydrated electron decay. *J. Photochem. Photobiol. Chem.* 133: 159–167.

52. Tsentalovich, Y. P., J. J. Lopez, P. J. Hore, and R. Z. Sagdeev. 2002. Mechanisms of reactions of flavin mononucleotide triplet with aromatic amino acids. *Spectrochim. Acta A. Mol. Biomol. Spectrosc.* 58:2043–2050.

53. Borman, C. D., C. Wright, M. B. Twitchett, G. A. Salmon, and A. G. Sykes. 2002. Pulse radiolysis studies on galactose oxidase. *Inorg. Chem.* 41:2158–2163.

54. Morozova, O. B., A. V. Yorkovskaya, H. M. Vieth, and R. Z. Sagdeev. 2003. Intramolecular electron transfer in tryptophan-tyrosine peptide in photoinduced reactions in aqueous solution. *J. Phys. Chem. B.* 107: 1088–1096.

55. Sherin, P. S., O. A. Snytnikova, and Y. P. Tsentalovich. 2004. Tryptophan photoionization from prefluorescent and fluorescent states. *Chem. Phys. Lett.* 391:44–49.

56. Tsentalovich, Y. P., O. A. Snytnikova, and R. Z. Sagdeev. 2004. Properties of excited states of aqueous tryptophan. *J. Photochem. Photobiol. Chem.* 162:371–379.

57. Eisinger, J., B. Feuer, and A. A. Lamola. 1969. Intramolecular singlet excitation transfer. Applications to polypeptides. *Biochemistry.* 8: 3908–3914.

58. Carvalho, A. S., A. M. Santos, M. T. Neves-Petersen, S. B. Petersen, M. R. Aires-Barros, and E. P. Melo. 2004. Conformational states of HRPA1 induced by thermal unfolding: effect of low molecular solutes. *Biopolymers.* 75:173–186.

59. Østergaard, L., A. K. Abelskov, O. Mattsson, and K. G. Welinder. 1996. Structure and organ specificity of an anionic peroxidase from Arabidopsis thaliana cell suspension culture. *FEBS Lett.* 398:243–247.